Small-Angle X-Ray and Neutron Scattering by Polymethylene, Polyoxyethylene, and Polystyrene Chains

D. Y. Yoon and P. J. Flory*

Department of Chemistry, Stanford University, Stanford, California 94305.
Received December 2, 1975

ABSTRACT: The angular dependence of the intensity of radiation scattering is computed for polymethylene, polyoxyethylene, and polystyrene chains over the range $0 < \mu < 0.3$ Å^{-1}, where $\mu = (4\pi/\lambda) \sin(\vartheta/2)$. The scattering functions $F_x(\mu)$, corresponding to $I\mu^2$ where I is the intensity, are developed for chains of x repeating units in terms of the even moments $\langle r_{ij}^{2p} \rangle$ of the separation distance between pairs of the units i and j, these moments $\langle r_{ij}^{2p} \rangle$ up to $p = 4$ being evaluated on the basis of realistic rotational isomeric models. The scattering functions, the convergence of which was confirmed by Monte Carlo calculations, increase monotonically with μ, rapidly at first and then very slowly as μ increases beyond ~0.05 Å^{-1}. The rate of increase in $F_x(\mu)$ beyond $\mu \approx 0.05$ Å^{-1} depends on configurational features of the chains, being smallest for POE and largest for PS chains. The theoretical scattering functions are in agreement with experimental results of small-angle neutron and x-ray scattering by PM in the molten state and by PS in the bulk and in solution. The inadequacies of the Debye equation, and of calculations based on artificial models in general, for $\mu >$ ~0.05 Å^{-1}, are pointed out.

The angular dependence of radiation scattering by polymer molecules when well separated one from another by dispersion in a medium of different scattering power is intimately related to the chain configuration.[1,2] The relationship most widely used as a basis for analysis of this angular dependence is the Debye equation[2]

$$P(\mu) = (2/v^2)(v - 1 + e^{-v}) \tag{1}$$

that expresses the ratio $P(\mu)$ of the intensity scattered at an angle ϑ to the scattered intensity at $\vartheta = 0$ as a function of v defined by[3]

$$v = \mu^2 \langle s^2 \rangle \tag{2}$$

where $\langle s^2 \rangle$ is the mean-squared radius of gyration and $\mu = (4\pi/\lambda) \sin(\vartheta/2)$ is the magnitude of the difference between incident and scattered wave vectors, λ being the wavelength in the scattering medium. The Debye equation rests on two assumptions:[2] (i) that the mean-squared distance $\langle \mathrm{r}_{ij}^2 \rangle$ between units i and j is proportional to the number $t = |i - j|$ of units separating the scattering centers i and j, and (ii) that the density distribution $W(\mathbf{r}_{ij})$ for vector $\mathbf{r}_{ij}$ is Gaussian (rather, that the Fourier transform of $W(\mathbf{r}_{ij})$ is Gaussian).[2] For random chains these assumptions hold at sufficiently small values of μ, i.e., over the light-scattering range or for x-ray scattering at very small angles. For values of μ^2 less than $\langle s^2 \rangle^{-1}$, eq 1 reduces to the universal relationship between the angular dependence of scattering and the radius of gyration, regardless of particle shape. With increase in scattering angle, or in μ, the scattering function depends progressively on correlations between pairs of units separated by smaller numbers t of units. For sequences with $t <$ 100 to 200, both assumptions (i) and (ii) fail.

The correlation distances that account for the major contributions to $P(\mu)$ for $\mu >$ ~0.03 Å^{-1} depend on the structure-related configurational characteristics of the chains under consideration. They cannot be generalized through representation by an artificial model. The scattering function in this range assumes special importance inasmuch as it reflects peculiarities of the particular chain under consideration. The advent of neutron scattering[4-11] at small angles as a useful technique for investigating the configurations of polymer chains has enhanced interest in the interpretation of $P(\mu)$ in this range.

Neutron scattering by molten polymethylene[10] and by amorphous polystyrene,[7,9] with contrast provided by deuteration of either "host" or "guest" molecules, failed to reveal significant departures from the Debye equation out to values of μ as great as 0.1 to 0.2 Å^{-1}. Theoretical calculations based on realistic models lead unambiguously to the conclusion that both assumptions (i) and (ii) are seriously in error in the relevant range of sequence lengths t. The conjecture that adherence to the Debye equation signified Gaussian behavior down to short sequences of the chains is therefore incorrect. Rather, the approximate agreement obtained should be regarded as fortuitous, being due to partial compensation of departures from one assumption by departures from the other, as we show here.

In other instances major departures from eq 1 are observed. The small-angle scattering of both X-rays and neutrons by syndiotactic poly(methyl methacrylate) affords a striking example.[5,12,13] The product $I\mu^2$, where I is the scattering intensity, passes through a maximum with μ in the vicinity of $\mu = 0.1$ Å^{-1}, instead of increasing monotonically with μ as required by eq 1.

In order to clarify these diverse dependences of the scattering function on μ, we examine in this paper the configurational characteristics of relatively short sequences within long chains of polymethylene (PM), polyoxyethylene (POE), and polystyrene (PS) chains, and, then, their contributions to the scattering functions.

Scattering Theory

The scattering function for a system of independent molecules oriented at random, each molecule being composed of $x + 1$ identical units, is given by

$$P(\mu) = (x + 1)^{-2} \sum_{i,j} \left\langle \frac{\sin(\mu r_{ij})}{\mu r_{ij}} \right\rangle \tag{3}$$

where r_{ij} is the distance between the units i and j and the angle brackets denote the statistical mechanical average over all configurations of the chain. This equation rests on the assumption that the structural unit may be treated as a point scatterer. The term $\langle (\mu r_{ij})^{-1} \sin(\mu r_{ij}) \rangle$ can be expanded as a series in the even moments $\langle r_{ij}^{2p} \rangle$ *of* r_{ij}, and for sufficiently long chains these moments may be replaced by $\langle r_t^{2p} \rangle$, without regard for the location of the sequence of $t = |i - j|$ units within the chain.[13,14] Then, the scattering function $F_x(\mu)$ defined as follows

$$F_x(\mu) = (x + 1)\mu^2 p(\mu)$$

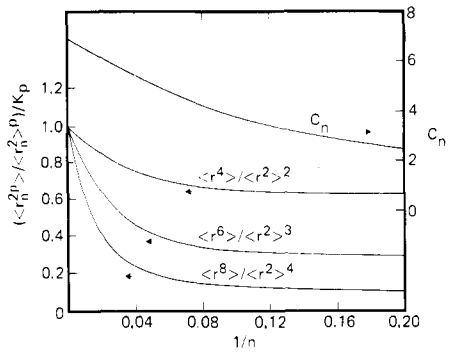

Figure 1. The characteristic ratio $C_n = \langle r_n^2\rangle/nl^2$ (right-hand ordinate scale) and relative values of the moment ratios $\langle r_n^{2p}\rangle/\langle r_n^2\rangle^p$ (left-hand ordinate scale) for PM chains plotted against $1/n$. The factors K_p are $^5/_3$, $^{35}/_9$, and $^{35}/_3$ for $p = 2$, 3, and 4, respectively.

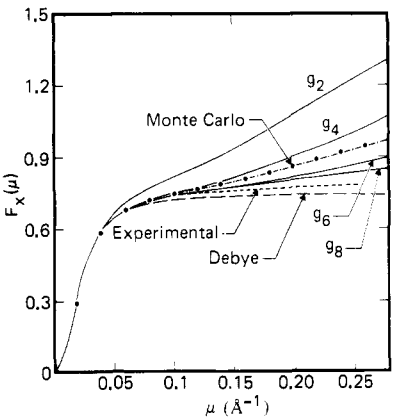

Figure 2. Scattering functions $F_x(\mu)$ (proportional to $I\mu^2$) plotted against μ for PM chains of 1000 skeletal bonds. The curves labeled "g_2", etc., were calculated from eq 4 truncated at g_2, etc., respectively. Monte Carlo calculations are shown by filled circles approximated by dash–dot curve. The Debye function is shown by the long-dashed curve. Experimental results of Fischer and co-workers on neutron scattering are represented by the short-dashed curve.

simplifies to[13,14]

$$F_x(\mu) = \mu^2 + 2\mu^2(x+1)^{-1}\sum_{t=1}^{x}(x+1-t)\left\langle\frac{\sin(\mu r_t)}{\mu r_t}\right\rangle$$

$$= \mu^2 + 2\mu^2(x+1)^{-1}\sum_{t=1}^{x}(x+1-t)\times$$
$$\exp(-\mu^2\langle r_t^2\rangle/6)[1 + g_{4;t}(\mu^2\langle r_t^2\rangle/3)^2 +$$
$$g_{6;t}(\mu^2\langle r_t^2\rangle/3)^3 + g_{8;t}(\mu^2\langle r_t^2\rangle/3)^4 + \ldots] \quad (4)$$

where

$$g_{4;t} = -2^{-3}[1 - 3\langle r_t^4\rangle/5\langle r_t^2\rangle^2]$$
$$g_{6;t} = -2^{-4}[(1 - 3\langle r_t^4\rangle/5\langle r_t^2\rangle^2) - {}^1/_3(1 - 9\langle r_t^6\rangle/35\langle r_t^2\rangle^3)]$$
$$g_{8;t} = -2^{-6}[(1 - 3\langle r_t^4\rangle/5\langle r_t^2\rangle^2) - {}^2/_3(1 - 9\langle r_t^6\rangle/35\langle r_t^2\rangle^3) + {}^1/_6(1 - 3\langle r_t^8\rangle/35\langle r_t^2\rangle^4)] \quad (5)$$

etc.[15] This scattering function may be compared with $I\mu^2$ observed experimentally.

Numerical Calculations

Polymethylene. Geometrical parameters and the statistical weight matrix used previously for the representation of this chain[2,16] were employed in the calculations presented here. First- and second-order statistical weights were assigned the values $\sigma = 0.54$ and $\omega = 0.088$, respectively, these being appropriate for a temperature of 140 °C.[16] The carbon atom was treated as a point scatterer representing the CH_2 group. The even moments $\langle r_n^{2p}\rangle$ with $p = 1$–4 were computed using matrix generation methods[2,17] for chains of n skeletal bonds and, hence, of $n + 1$ units. Previous computations have shown that $\langle r_t^2\rangle$ for a sequence of t units within long PM chains is virtually equal to $\langle r_n^2\rangle$ for the chain CH_3–$(CH_2)_n$–H with $n = t$.[14] This equivalence holds in good approximation, regardless of the location of the t-bond sequence within the long chain. Hence, we identify the $\langle r_t^{2p}\rangle$ for sequences with the computed moments $\langle r_n^{2p}\rangle$ for a chain having a total of $n = t$ bonds. Computations were carried out for $n = 2$ to 200 bonds.

In Figure 1 the characteristic ratio $C_n = \langle r_n^2\rangle/nl^2$ is plotted against $1/n$ on the right-hand ordinate scale. The moment ratios $\langle r_n^4\rangle/\langle r_n^2\rangle^2$, $\langle r_n^6\rangle/\langle r_n^2\rangle^3$, and $\langle r_n^8\rangle/\langle r_n^2\rangle^4$ are referred to the left-hand scale; scales are adjusted by the factors K_p required to render the intercepts coincident and equal to unity for each ratio. The monotonic decrease of C_n with $1/n$ demonstrates the deviation from assumption (i) of the Debye theory as applied to finite sequences. Departures of the ratio $\langle r_n^4\rangle/\langle r_n^2\rangle^2$, required for the evaluation of $g_{4;n}$, from its limiting value, $^5/_3$, with decrease in t, are indicative of the degree to which the distribution $W(\mathbf{r}_n)$ deviates from the Gaussian distribution assumed in the derivation of the Debye equation, i.e., from assumption (ii). Departures of the values of $\langle r_n^6\rangle/\langle r_n^2\rangle^3$ and $\langle r_n^8\rangle^4/\langle r_n^2\rangle^4$ from their limiting values, $^{35}/_9$ and $^{35}/_3$, respectively, offer further indications of the non-Gaussian character of the distribution function $W(\mathbf{r}_n)$ for chains of finite length. The values of C_n, $\langle r_n^4\rangle/\langle r_n^2\rangle^2$, etc., for $n > 200$, required for the calculations below, were readily evaluated with high accuracy by extrapolation of results for $n \leq 200$.

Scattering functions $F_x(\mu)$ for a polymethylene chain of 1000 skeletal bonds ($x = n = 1000$) are shown in Figure 2 for $\mu = 0$ to 0.3 Å^{-1}. The functions were calculated according to eq 4 truncated at g_2, etc., as indicated with each curve. The required moments $\langle r_t^{2p}\rangle$ for sequences of t units were assigned the values computed for chains of $n = t$ bonds, the error arising from this identification being negligible as pointed out above. The curve labeled "g_2" rises much above the Debye function represented by the long-dashed line. The "g_2" curve takes account of the variation of C_n with n (see Figure 1), thereby correcting for noncompliance with condition (i) above. The effect is large. Correction for the non-Gaussian character of the distribution by incorporation of the terms in $g_{4;t}$, $g_{6;t}$, and $g_{8;t}$ in eq 4 progressively diminishes $F_x(\mu)$ in the range of large μ. The difference between $F_x(\mu)$ calculated from the series truncated at g_6 and at g_8 indicates incomplete convergence.

In view of the impracticability of evaluating higher moments, we resorted to Monte Carlo calculations of $\langle(\mu r_t)^{-1}\sin(\mu r_t)\rangle$ for $t < 100$, in order to ascertain the limiting form of the function $F_x(\mu)$. For sequences with $t > 100$, the series in eq 4 converges adequately at g_8, and hence was used for evaluation of this portion of the sum over t. These longer sequences ($t > 100$) make only a small contribution to $F_x(\mu)$ for $\mu > 0.05$ Å^{-1}, the range of main interest here.

The Monte Carlo calculations were carried out as described previously,[18] the basis being the same rotational isomeric state scheme used above for the analytical evaluation of moments. That is, the conformation of each bond was assigned from computer-generated random numbers with ranges apportioned according to conditional probabilities $q_{\zeta\eta;i}$ for bond i in state η when bond $i - 1$ is in state ζ.[18] These conditional probabilities were calculated from the a priori probabilities $p_{\zeta\eta;i}$ and $p_{\zeta;i-1}$ according to the relation[2]

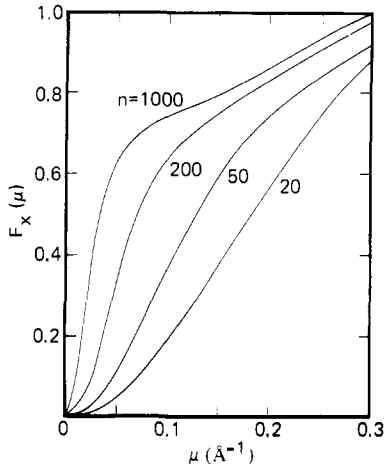

Figure 3. The scattering function $F_x(\mu)$ for PM chains with n = 20, 50, 200, and 1000 bonds.

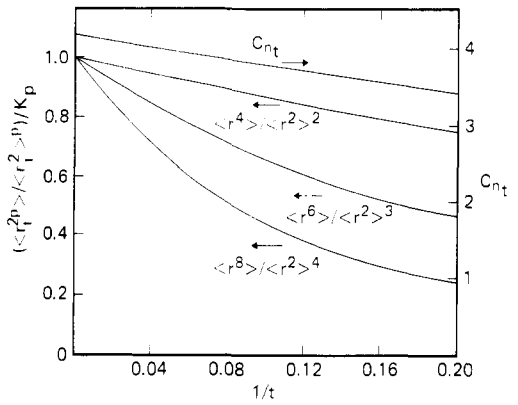

Figure 4. The characteristic ratio $C_{n_t} = \langle r_t^2\rangle/3tl^2$, l being 1.43 Å, and the moment ratios $\langle r_t^{2p}\rangle/\langle r_t^2\rangle^p$ for POE chains of t repeating units centered within chains of t + 200 units plotted against $1/t$. See legend to Figure 1 for values of K_p.

$$q_{\zeta\eta;i} = p_{\zeta\eta;ii}/p_{\zeta;i-1} \tag{6}$$

the a priori probabilities being evaluated using the same rotational isomeric state scheme and the same statistical weight parameters as above.[2] The value of r_t for the conformation thus generated yields $(\mu r_t)^{-1}\sin(\mu r_t)$.

Averages over sets of 1000 conformations for each value of t in the range t = 3–100 together with the fixed values of $\langle(\mu r_t)^{-1}\sin(\mu r_t)\rangle$ for t = 1 and 2, and with the higher terms according to eq 4 for $t > 100$, yielded the points shown as filled circles in Figure 2. The dash–dot curve described by these points lies above the "g_6" and "g_8" curves. Hence, we infer that higher terms in eq 4, if included, would reverse the trends noted above. The "Monte Carlo" curve, taken to be the most accurate representation of the scattering functions for the PM chain, is nevertheless closer to the Debye function than to the "g_2" curve which, as noted above, takes account only of the failure of assumption (i) according to which $\langle r_t^2\rangle$ is assumed to be proportional to t. Thus, the error arising from this assumption is compensated to a major degree by the departure from assumption (ii) that the distribution is Gaussian.

Experimental results of Fischer and co-workers[10] deduced from neutron scattering measurements on molten mixtures of protonated PM in the deuterated host at 140 °C are represented by the short-dashed line in Figure 2. It lies between the Debye and Monte Carlo curves, but is closer to the former. The theoretical (Monte Carlo) values of

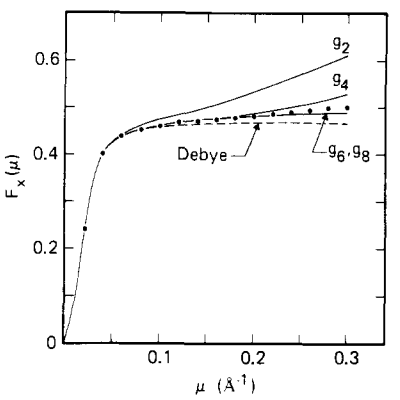

Figure 5. The scattering functions $F_x(\mu)$ plotted against μ for the POE chain of 1000 repeating units. The filled circles represent Monte Carlo calculations. See the legend to Figure 2.

$F_x(\mu)$ exceed the experimental results by about 10% at μ = 0.2 Å^{-1}. This difference is well within the limits of error in the experimental measurements at large values of μ where the difference between the observed intensities for the sample and the reference (fully deuterated) is small.

The calculated scattering functions $F_x(\mu)$ for PM chains with x = 20, 50, 200, and 1000 are compared in Figure 3. All calculations were carried out according to eq 4 with the terms $\langle(\mu r_t)^{-1}\sin(\mu r_t)\rangle$ evaluated by Monte Carlo calculations for $t \leq 100$ and by series expansion truncated at $g_{8;t}$ for $t > 100$. The convergence of the scattering functions for x = 200 and 1000 with increase in μ reflects the fact that comparatively short sequences make the main contribution to the scattering function when μ is large.[29]

Polyoxyethylene. Calculations were carried out using the geometrical parameters, rotational states, and associated statistical weight matrices given previously[19,20] for POE. Statistical weight parameters were assigned values, appropriate for a temperature of 60 °C, as follows: σ = 0.26 and σ' = 1.90 for rotations about C–O and C–C bonds, respectively, and second-order parameters ω = 0 and ω' = 0.60 for bond pairs C–O–C and O–C–C, respectively. These values were deduced principally from experimental results on chain dimensions and dipole moments, and on the temperature coefficients of these quantities.[19,20]

The skeletal oxygen atom was treated as the point scatterer representing the CH_2CH_2O unit. The even moments $\langle r_t^{2p}\rangle$ with p = 1 to 4 were computed for sequences of t units (n = 3t bonds) centered within a chain comprising 100 + t + 100 units in the same manner as described previously for poly(methyl methacrylate) chains.[13] The range t = 2 to 100 was covered by direct calculation. Values for $t >$ 100 were evaluated by extrapolation.

The characteristic ratios $C_{n_t} = \langle r_t^2\rangle/3tl^2$ for the sequence of t units within the long chain are plotted against $1/t$ in Figure 4; the subscript n_t is appended to denote reference to a sequence of n_t = 3t bonds within a longer chain. Values of $\langle r_t^4\rangle/\langle r_t^2\rangle^2$, $\langle r_t^6\rangle/\langle r_t^2\rangle^3$, and $\langle r_t^8\rangle/\langle r_t^2\rangle^4$ are shown also in Figure 4. The monotonic decrease of C_{n_t} with $1/t$ describes the departure from assumption (i) of the Debye treatment. Decreases of $\langle r_t^4\rangle/\langle r_t^2\rangle^2$, $\langle r_t^6\rangle/\langle r_t^2\rangle^3$, and $\langle r_t^8\rangle/\langle r_t^2\rangle^4$ below their limiting values indicate the deviations from assumption (ii). These departures are less severe than for polymethylene. Associated with this observation is the fact that the ratios $\langle r_t^4\rangle/\langle r_t^2\rangle^2$, $\langle r_t^6\rangle/\langle r_t^2\rangle^3$, and $\langle r_t^8\rangle/\langle r_t^2\rangle^4$ for POE conform to values for the equivalent freely jointed model chain down to smaller values of n_t, or n, than holds for PM chains (see the Appendix).

The scattering functions $F_x(\mu)$ for POE chain of 1000

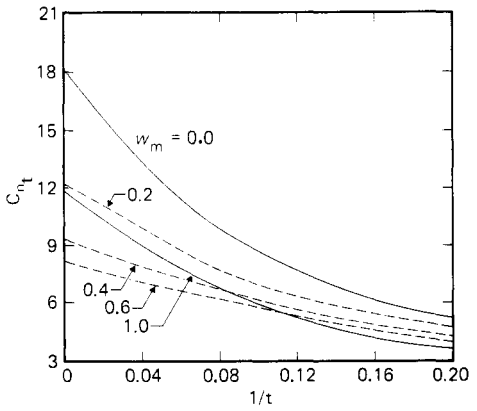

Figure 6. The characteristic ratios $C_{n_t} = \langle r_t^2 \rangle / 2tl^2$ plotted against $1/t$ for PS chains composed of t repeating units situated within chains of $t + 200$ units. The stereochemical composition of PS chains is indicated by w_m, the average fraction of meso dyads.

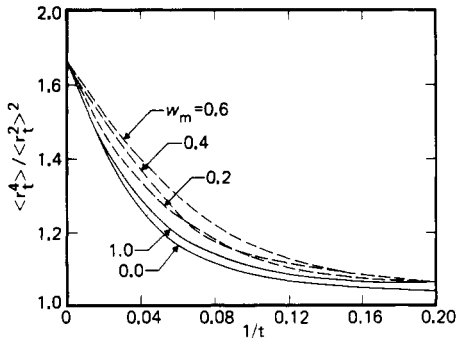

Figure 7. The ratios $\langle r_t^4 \rangle / \langle r_t^2 \rangle^2$ plotted against $1/t$ for PS chains of t repeating units situated within longer chains.

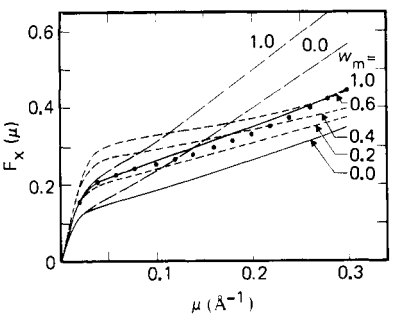

Figure 8. The scattering functions $F_x(\mu)$ plotted against μ for PS chains of 1000 repeating units. The long-dashed curves were calculated from eq 4 truncated at g_2 for isotactic and syndiotactic chains. The curves truncated at g_8 are shown by solid lines for isotactic and syndiotactic chains and by short-dashed lines for atactic chains. The filled circles represent Monte Carlo calculations for isotactic chains.

units are plotted against μ in Figure 5. The series in eq 4 was truncated at the terms indicated. Results for truncation at g_6 and g_8 are virtually coincident, and hence are represented by the same curve. Convergence of the series throughout the range of $\mu < 0.3$ Å^{-1} is thus demonstrated. This is further confirmed by the close agreement of Monte Carlo calculations, shown by the filled circles in Figure 5, with the same curve. These calculations were carried out following the procedure adopted above for PM chains. The values of $\langle (\mu r_t)^{-1} \sin (\mu r_t) \rangle$ were obtained by averaging over sets of 1000 Monte Carlo chains consisting of $100 + t + 100$ units (see above) for $t \leq 50$ units and by series expansion truncated at g_8 for $t > 50$.

The theoretical scattering function $F_x(\mu)$ for POE chains exhibits a smaller departure from the Debye equation than the PM series. Experimental results with which to compare these calculations are not available.

Polystyrene. The conformational characteristics of polystyrene chains can be represented in good approximation by combinations of the two rotational isomeric states located at $\varphi_t = 10°$ and $\varphi_g = 110°$, respectively,[21] the bond rotational angles being measured in the sense depending on the chirality of the bond.[22] Conformations in the $\bar{g}$ domain generated by rotations of opposite sense ($\varphi \approx -120°$) are of excessively high energy owing to severe steric interactions involving the planar phenyl group, and, hence, may be ignored.[21] Geometrical parameters and statistical weights were taken from ref 21 for a temperature of 300 K.

The substituted carbon atom C^α was treated as the point scatterer representing the repeating unit CH_2–$CH(C_6H_5)$. The even moments $\langle r_t^{2p} \rangle$ were computed for chains of t units centered within a larger chain of $100 + t + 100$ units. The range $t = 2$ to 200 was covered by direct calculations for all of the moments up to $\langle r_t^8 \rangle$ for the stereoregular isotactic and syndiotactic chains, and up to $\langle r_t^4 \rangle$ for the atactic chains. Atactic chains with Bernoullian sequence distributions were generated by Monte Carlo methods. Three sets of ten chains each were generated for expectations w_m of meso dyads of 0.2, 0.4, and 0.6, respectively.

Owing to the excessive computing time necessary for evaluation of $\langle r_t^6 \rangle$ and $\langle r_t^8 \rangle$ by Monte Carlo methods, these higher moments for the atactic chains were approximated by employing the "equivalent freely jointed" model chain used previously for atactic poly(methyl methacrylate) chains.[13] From the given values of $\langle r_t^4 \rangle / \langle r_t^2 \rangle^2$ for the atactic chain of t monomer units, the number of equivalent freely jointed bonds, n^*, was obtained from eq A-1 in the Appendix. Then, $\langle r_t^6 \rangle / \langle r_t^2 \rangle^3$ and $\langle r_t^8 \rangle / \langle r_t^2 \rangle^4$ were evaluated by inserting n^* into eq A-2 and A-3. According to corresponding calculations for the isotactic and syndiotactic chains, the error in this indirect procedure is less than 10% for all chain lengths.

In Figure 6, $C_{n_t} = \langle r_t^2 \rangle / 2tl^2$, $n_t = 2t$ being the number of skeletal bonds, is plotted against $1/t$ for polystyrene chains of the different stereoregularities as denoted by the average fractions w_m of meso dyads. The values of $\langle r_t^4 \rangle / \langle r_t^2 \rangle^2$ are shown in Figure 7. The variations of $\langle r_t^6 \rangle / \langle r_t^2 \rangle^3$ and $\langle r_t^8 \rangle / \langle r_t^2 \rangle^4$ with t for stereoregular isotactic and syndiotactic chains closely resemble the corresponding results for PM and POE chains; hence, they are not shown here. The values of C_{n_t}, $\langle r_t^4 \rangle / \langle r_t^2 \rangle^2$, etc., for $t > 200$ are again reliably obtained by extrapolation.

The scattering functions $F_x(\mu)$ for PS chains of 1000 repeating units are plotted against μ in Figure 8. For the isotactic ($w_m = 1.0$) and syndiotactic ($w_m = 0.0$) chains, the functions truncated at g_2 and g_8 are shown by long dashed and solid curves, respectively. Functions calculated with truncations at g_8 for three atactic chains with $w_m = 0.2$, 0.4, and 0.6, respectively, are shown by short-dashed curves. The differences between the curves truncated at g_2 and g_8 shown for isotactic and syndiotactic chains in Figure 8 (and also for atactic chains though not shown here) are much larger than those for PM and POE chains (see Figures 2 and 5). This is due to the fact that the distributions of chain vectors $\mathbf{r}_t$ for relatively short sequences of PS chains are strongly non-Gaussian.

The adequacy of the convergence of the curves truncated at g_8 was examined by carrying out the Monte Carlo calculations for isotactic PS shown by filled circles in Figure 8. These data were calculated in the manner described above for PM and POE chains, the values of $\langle (\mu r_t)^{-1} \sin (\mu r_t) \rangle$

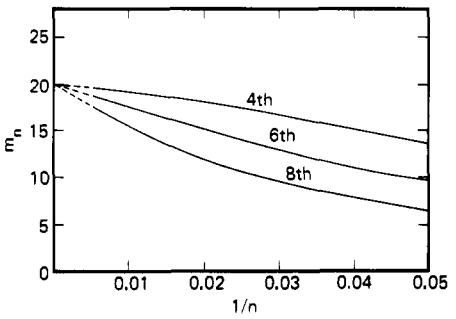

Figure 9. The values of m_n obtained for PM chains from $\langle r^4\rangle/\langle r^2\rangle^2$, $\langle r^6\rangle/\langle r^2\rangle^3$, and $\langle r^8\rangle/\langle r^2\rangle^4$, respectively, plotted against $1/n$, where n is the number of skeletal bonds.

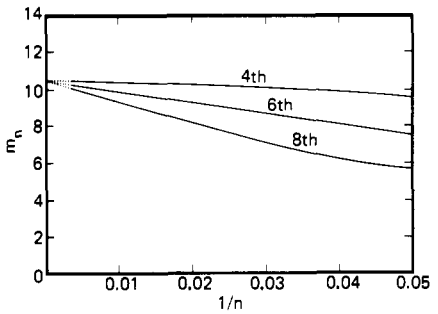

Figure 10. The values of m_n for POE chains calculated from the respective moment ratios plotted against $1/n$.

being evaluated by averaging over 1000 Monte Carlo chains of $100 + t + 100$ units for $t \leq 50$ units. The close agreement of the "g_8" curve ($w_m = 1.0$) with the Monte Carlo results demonstrates adequate convergence, and lends support to the other calculations, likewise truncated at g_8, for values of $w_m < 1.0$.

The scattering function of $F_x(\mu)$ increases monotonically with μ for PS chains, for all stereochemical compositions measured by w_m. The slope of the increase for $\mu > 0.1$ Å^{-1} depends, however, upon the stereoregularity of the chain, being greater for the stereoregular isotactic and syndiotactic chains than for atactic chains.

The neutron scattering experiments on PS chains reported by Benoit and his co-workers[7] and also by Wignall et al.[9] indicate that $I\mu^2 \propto F_x(\mu)$ levels off with μ in the range $0.1 < \mu < 0.3$ Å^{-1}. Also the small-angle x-ray scattering by PS[23] and poly(*m*-bromostyrene) chains[24] in solutions exhibit the same trend. The latter polymer[25] resembles PS in its configurational characteristics. The stereochemical composition of conventional atactic PS is not well characterized, but it is generally believed to be in the range $w_m = 0.4 \pm 0.1$.[26] The scattering function $F_x(\mu)$ for $w_m = 0.4$ shown in Figure 8 increases slowly with μ for $\mu > 0.1$ Å^{-1}. Detection of this small rise in $F_x(\mu)$ may have been beyond the limits of errors in the experiments cited.

Acknowledgment. This work was supported by the National Science Foundation, Grant No. DMR-73-07655 A02.

Appendix

Equivalent Freely Jointed Model Chain. For the model chain composed of n^* freely jointed bonds,[27]

$$\frac{\langle r^4\rangle}{\langle r^2\rangle^2} = \frac{5}{3} - \frac{2}{3n^*} \tag{A-1}$$

$$\frac{\langle r^6\rangle}{\langle r^2\rangle^3} = \frac{35}{9} - \frac{14}{3n^*} + \frac{16}{9n^{*2}} \tag{A-2}$$

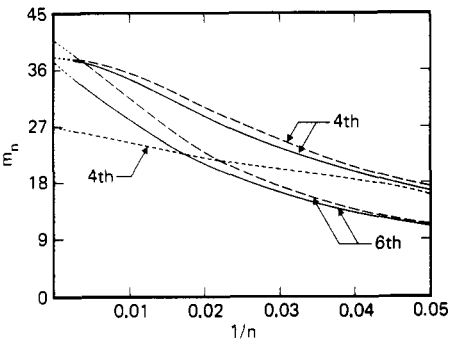

Figure 11. The values of m_n for PS chains calculated from the respective moments plotted against $1/n$. The full lines represent the isotactic chain, the long-dashed lines represent the syndiotactic chain, and the short-dashed line represents the atactic chain with $w_m = 0.4$.

$$\frac{\langle r^8\rangle}{\langle r^2\rangle^4} = \frac{35}{3} - \frac{28}{n^*} + \frac{404}{15n^{*2}} - \frac{48}{5n^{*3}} \tag{A-3}$$

etc. If we consider a bond of the freely jointed chain to be equivalent to m bonds of the real chain, then a real chain of n bonds will be equivalent to a freely jointed chain having $n^* = n/m$ bonds. Substitution in eq A-1, -2, and -3 gives

$$\frac{5}{3} - \frac{\langle r^4\rangle}{\langle r^2\rangle^2} = \frac{2}{3}\frac{m}{n} \tag{A-4}$$

$$\frac{35}{9} - \frac{\langle r^6\rangle}{\langle r^2\rangle^3} = \frac{14}{3}\frac{m}{n}\left(1 - \frac{8}{21}\frac{m}{n}\right) \tag{A-5}$$

$$\frac{35}{3} - \frac{\langle r^8\rangle}{\langle r^2\rangle^4} = 28\frac{m}{n}\left(1 - \frac{101}{105}\frac{m}{n} + \frac{12}{35}\frac{m^2}{n^2}\right) \tag{A-6}$$

The value of m that establishes correspondence between the equivalent and real chains in the long-chain limit may be obtained graphically in the following manner. Using the fourth moments we plot $m_n = \frac{3}{2}n(\frac{5}{3} - \langle r^4\rangle/\langle r^2\rangle^2)$ against $1/n$ and extrapolate to $1/n = 0$. Similarly, using the numerical values for the sixth and eighth moments, we plot $m_n = \frac{3}{14}n(\frac{35}{9} - \langle r^6\rangle/\langle r^2\rangle^3)$ and $(n/28)(\frac{35}{3} - \langle r^8\rangle/\langle r^2\rangle^4)$, respectively, against $1/n$. Treatment of data in this manner is shown in Figures 9–11 for the three polymers.

Intercepts of m_n at $1/n = 0$ from the fourth, sixth, and eighth moments yield $m \approx 20$ for PM chains, $m \approx 10.5$ for POE, and $m \approx 37.5$, 39, and 27 for isotactic, syndiotactic, and atactic ($w_m = 0.4$) PS chains, respectively. These limiting values of m for PM and POE are in good agreement with those obtained from the results of similar analyses[18,28] of tensor moments formed from vector **r**. In the analysis of the tensor moments account is taken of the persistence of the vector $\mathbf{a} \equiv \langle \mathbf{r} \rangle$ and the asymmetric spatial characteristics of the distribution function $W(\mathbf{r})$ when referenced to the polymer chain.

References and Notes

(1) P. Debye, *J. Phys. Chem.*, **51**, 18 (1947).
(2) P. J. Flory, "Statistical Mechanics of Chain Molecules", Interscience, New York, N.Y., 1969, pp 340–350.
(3) P. J. Flory and R. L. Jernigan, *J. Am. Chem. Soc.*, **90**, 3182 (1968).
(4) R. G. Kirste, W. A. Kruse, and J. Schelten, *Makromol. Chem.*, **162**, 299 (1972).
(5) R. G. Kirste, W. A. Kruse, and K. Ibel, *Polymer*, **16**, 120 (1975).
(6) H. Benoit, D. Decker, J. S. Higgins, C. Picot, J. P. Cotton, B. Farnoux, G. Jannink, and R. Ober, *Nature (London), Phys. Sci.*, **245**, 13 (1973).
(7) J. P. Cotton, D. Decker, H. Benoit, B. Farnoux, J. Higgins, G. Jannink, R. Ober, C. Picot, and J. des Cloizeaux, *Macromolecules*, **7**, 863 (1974).
(8) D. G. H. Ballard, J. Schelten, and G. D. Wignall, *Eur. Polym. J.*, **9**, 965 (1973).
(9) G. D. Wignall, D. G. H. Ballard, and J. Schelten, *Eur. Polym. J.*, **10**, 861 (1974).
(10) E. W. Fischer, J. H. Wendorff, M. Dettenmaier, G. Leiser, and I. Voigt-

Martin, *Polym. Prepr., Am. Chem. Soc., Div. Polym. Chem.*, **15**(2), 8 (1974).
(11) G. Leiser, E. W. Fischer, and K. Ibel, *J. Polym. Sci., Polym. Lett.*, **13**, 39 (1975).
(12) R. G. Kirste, *Makromol. Chem.*, **101**, 91 (1967).
(13) D. Y. Yoon and P. J. Flory, *Polymer*, **16**, 645 (1975).
(14) Y. Fujiwara and P. J. Flory, *Macromolecules*, **3**, 288 (1970).
(15) See ref 2, pp 309–311.
(16) A. Abe, R. L. Jernigan, and P. J. Flory, *J. Am. Chem. Soc.*, **88**, 631 (1966).
(17) P. J. Flory, *Macromolecules*, **7**, 381 (1974).
(18) D. Y. Yoon and P. J. Flory, *J. Chem. Phys.*, **61**, 5366 (1974).
(19) See ref 2, pp 165–172.
(20) J. E. Mark and P. J. Flory, *J. Am. Chem. Soc.*, **88**, 3702 (1966).
(21) D. Y. Yoon, P. R. Sundararajan, and P. J. Flory, *Macromolecules*, **8**, 776 (1975).
(22) P. J. Flory, P. R. Sundararajan, and L. C. DeBolt, *J. Am. Chem. Soc.*, **96**, 5015 (1974).
(23) H. Durchschlag, O. Kratky, J. W. Breitenbach, and B. A. Wolf, *Monatsh. Chem.*, **101**, 1462 (1970).
(24) H. Durchschlag, G. Puchwein, O. Kratky, J. W. Breitenbach, and O. F. Olaj, *J. Polym. Sci., Part C*, **31**, 311 (1970).
(25) D. Y. Yoon and P. J. Flory, in preparation.
(26) L. F. Johnson, F. Heatley, and F. A. Bovey, *Macromolecules*, **3**, 175 (1970).
(27) See ref 2, pp 307–314.
(28) A. Abe, in preparation.
(29) NOTE ADDED IN PROOF: Since this paper was submitted, we have learned that similar calculations on polymethylene chains have been carried out by Z. Zierenberg, D. K. Carpenter, and J. H. Hsieh. Our results are in agreement with theirs, which will appear in the *J. Polym. Sci., Polym. Symp.*

II. Small-Angle Neutron and X-Ray Scattering by Poly(methyl methacrylate) Chains

D. Y. Yoon and P. J. Flory*

Department of Chemistry, Stanford University, Stanford, California 94305.
Received December 2, 1975

ABSTRACT: Scattering functions describing the angular dependence of the intensity of radiation scattering by poly(methyl methacrylate) (PMMA) chains are calculated on the basis of an appropriate rotational isomeric state model. Numerical calculations are carried out, with main emphasis on the range $0.05 < \mu < 0.5$ Å^{-1}, where $\mu = (4\pi/\lambda) \sin(\vartheta/2)$, by evaluating $\langle(\mu r_{ij})^{-1} \sin(\mu r_{ij})\rangle$ for pairs of scattering groups i and j as the averages for 1000 Monte Carlo chains. Errors incident upon truncation of series expansions of this quantity for large magnitudes of the scattering vector μ are thus avoided. The theoretical scattering function $F_x(\mu) \propto I\mu^2$ exhibits two maxima, in harmony with experimental results of Kirste on small-angle x-ray scattering by syndiotactic PMMA chains in solution. The point scatterer approximation according to which the scattering by each repeating unit is identified with the location of the α carbon is inappropriate for neutron scattering by *H*-PMMA dispersed in *D*-PMMA host. Calculations for separate scattering loci centered in CH_3 and CH_2 groups differ considerably at large μ from those carried out in the point scatterer approximation. They are in good agreement with experimental neutron scattering results. Thus, the validity of the rotational isomeric state analysis for comparatively short chain sequences is demonstrated.

In a recent paper[1] we presented theoretical computations on the intensity of radiation scattering by poly(methyl methacrylate) (PMMA) as a function of scattering angle ϑ over the range $0 < \mu < 0.3$ Å^{-1}, where $\mu = (4\pi/\lambda) \sin(\vartheta/2)$. The calculations were carried out according to eq 4 of the preceding paper[2] truncated at g_8. The required moments were computed on the basis of a rotational isomeric state scheme that is in harmony with the geometric characteristics and steric constraints in the PMMA chain and with detailed calculations of its conformational energy.[3] The theoretical scattering function $F_x(\mu)$, which is proportional to $I\mu^2$, where I is the scattering intensity, was found to increase monotonically with μ for isotactic PMMA. For predominantly syndiotactic PMMA, however, the calculated $F_x(\mu)$ exhibited a maximum at $\mu \approx 0.05$ Å^{-1} and a minimum at $\mu \approx 0.18$ Å^{-1}. These features of the variation of $F_x(\mu)$, or of $I\mu^2$, with μ and their dependence on the stereochemical configuration of PMMA were found to be in satisfactory qualitative agreement with the experimental results of small-angle neutron and x-ray scattering by PMMA chains in bulk and in solution, respectively, as reported by Kirste and co-workers.[4–6] The unusual appearance of a maximum in $F_x(\mu)$ had been misconstrued as evidence of helical sequences in solution or of ordered regions in the bulk polymers. In our previous paper[1] this maximum was shown, on the contrary, to be a direct consequence of the preference of racemic dyads of PMMA for the trans,trans conformation in the random coiled state together with the inequality of the skeletal bond angles at $-CH_2-$ and at the disubstituted C^α atom.

With respect to quantitative treatment of scattering in the range $\mu > \sim 0.10$ Å^{-1}, however, the preliminary calculations[1] are deficient in two respects: (i) truncation of the series expansion of the scattering function $F_x(\mu)$ at terms in $\langle r_t^8\rangle$ (see eq 4 of the preceding paper,[2] referred to hereafter as I), and (ii) representation of the repeating unit

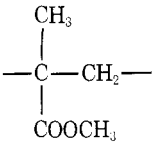

as a point scatterer located at the C^α atom. The latter approximation is especially inappropriate for neutron scattering by protonated (or deuterated) PMMA dispersed in a deuterated (or protonated) PMMA host. The scattering length of the CD_2 group for coherent scattering of neuterons is large compared to the vanishingly small value for CH_2. The distinction between deuterons and protons (or vice versa) therefore is the principal source of contrast, and hence these atoms (H or D) are the main loci of scattering. The methylene and methyl groups in which they are situated are appreciably displaced from C^α.

The point scatterer approximation should be more appropriate for small-angle x-ray scattering by PMMA chains in a solvent where the contrast in electron density between